

1 Correlation Scales of Digital Elevation Models in Developed Coastal 2 Environments

3
4 Christopher Small_a and Robert Sohn_b

5
6 _a *Lamont-Doherty Earth Observatory, Columbia University, Palisades, NY 10964*

7 _b *Woods Hole Oceanographic Institution, Woods Hole, MA 02543*

8 9 Abstract

10
11 Accuracy of digital elevation models (DEMs) often depends on how features of different
12 spatial scales are represented. Scale dependence is particularly important in low gradient
13 coastal environments where small vertical errors can affect large areas and where
14 representation of fine scale topographic features can influence how DEMs are used for
15 modeling inundation. It is commonly observed that different types of DEMs represent
16 larger, coarse-scale topographic features similarly, but differ in how they represent
17 smaller, finer-scale features. Spatial scale dependence of DEM accuracy can be
18 quantified in terms of the correlation scale (λ_c); the spatial wavelength above which
19 models agree with spectral coherency > 0.5 and below which they differ. We compare
20 cross spectral analyses of the GDEM2 and SRTM global DEMs with 14,572 LiDAR-
21 derived elevations along transects in diverse coastal environments of New York City.
22 Both global DEMs have positive bias relative to LiDAR ground elevations, but bias
23 (μ) and uncertainty (σ) of GDEM2 (μ : 8.1 m; σ : 7.6 m) are significantly greater than
24 those of SRTM (μ : 1.9 m; σ : 3.6 m). Cross-spectral coherency between GDEM2 and the
25 LiDAR DEM begins to roll-off at scales of $\lambda < \sim 3$ km, while coherency between SRTM
26 and the LiDAR DEM begins to roll-off at scales of $\lambda < \sim 1$ km. The correlation scale
27 below which coherency with LiDAR attains a signal to noise ratio of 1 is ~ 1 km for
28 GDEM2 and ~ 0.5 km for SRTM; closely matching the divergence scales where the
29 surface roughness of the land cover exceeds the roughness of the underlying terrain.

32

33

34 **Introduction**

35

36 Hazard assessments and inundation modeling of coastal areas rely heavily on both the
37 accuracy and resolution of digital elevation models (DEMs). In many coastal areas
38 global DEMs offer the most complete representation of coastal elevations and
39 morphology available. Two distinct classes of global DEM are currently in widespread
40 use: passive source stereographic models derived from optical imagery like the ASTER
41 GDEM2 (Abrams et al. 2010), and active source ranging models derived from synthetic
42 aperture radar like the SRTM (Farr et al. 2007). The accuracy of each model depends on
43 multiple factors related to the sensing modality, the procedure used to estimate
44 elevations, and the characteristics of the land surface (Farr et al. 2007; Lang and Welch
45 1999). The recent release of full resolution 30 m SRTM data for areas outside the US
46 (previously degraded to 90 m) prompts the question of how the accuracy and effective
47 spatial resolution of SRTM and GDEM2 compare, particularly in developed coastal
48 environments where they may be used for inundation modeling and hazard assessments.

49

50 The accuracy and resolution of DEMs in coastal environments, where there are relatively
51 small differences in elevation over large areas, are of special interest. At low elevations
52 and gradients the signal magnitude approaches the noise level of the measurements,
53 which can lead to large errors in inundation extent forecasts. This issue is particularly
54 important for developed coastal environments where the spatial extent of inundation can
55 have disproportionate consequences in terms of loss of life and property. There have been
56 several comparative analyses of global DEM vertical accuracy (e.g. (Gesch et al. 2012;
57 Meyer et al. 2012), (Tachikawa et al. 2011; Tadono et al. 2012), (Smith and
58 Sandwell 2003)). Some analyses have included coastal areas (e.g. (Gorokhovich and
59 Voustianiouk 2006), (Hvidegaard et al. 2012)), and some have incorporated land
60 cover/use information (e.g. (Gesch et al. 2012), (Hofton et al. 2006), (Carabajal and
61 Harding 2006)), but we are not aware of any that specifically consider the accuracy and
62 spatial resolution of global DEMs in developed coastal environments. As explained
63 below, the scale and diversity of land cover in developed coastal areas is fundamentally
64 different from most of the environments where previous studies have focused.

65

66 The objective of this analysis is to assess the accuracy and scale dependence of the
67 GDEM2 and SRTM global DEMs in developed coastal environments. We address the
68 issue by quantifying the scale dependence of the agreement between these global DEMs
69 and high-accuracy, high-resolution, LiDAR-derived elevations for a diverse variety of
70 coastal environments within New York City (NYC). We quantify the scale dependence
71 by using cross-spectral analysis to estimate the correlation scale (the length scale below
72 which two signals are uncorrelated) of each global DEM with a co-registered DEM and
73 digital surface model (DSM) derived from LiDAR. The LiDAR DEM (LDEM) and
74 DSM (LDSM) have been thoroughly validated throughout the study area, and thus
75 provide high-quality benchmarks for the analysis. We focus on quantifying the lateral
76 length-scale at which the agreement between two models becomes random. This is
77 complementary to, but distinct from, previous studies that used point-to-point

78 comparisons (e.g., GPS or fiducial) to measure the absolute accuracy of the global
79 DEMs. To our knowledge, the only scale-dependent analyses of global DEMs are those
80 of (Smith and Sandwell 2003) and (Rodriguez et al. 2006) but neither focus on
81 developed or coastal environments.

82

83

84 **Data**

85

86 The geological and geomorphic diversity of NYC includes a wide range of developed and
87 natural coastal environments and land cover/use types. Four of NYC's five boroughs are
88 islands. Included in NYC's 837 km of coastline are beaches, barrier islands, tidal
89 wetlands, estuarine marshes, rivers, channels and a variety of reinforced embankments on
90 the shores of New York Harbor, Long Island Sound, the Atlantic Ocean and the Hudson,
91 Harlem and East Rivers (Fig. 1).

92

93 The LiDAR DEM and DSM were produced from a 17-day airborne campaign conducted
94 by Sanborn Inc. in April 2010. The ALS-50 near infrared LiDAR instrument was flown
95 at an altitude of 1100 m with a scan angle of 28°. The 937 km² collection of 15 x 10⁹
96 elevation measurements results in a point density of 8 to 12 points/m². Comparison of
97 LiDAR elevations with 1722 survey elevations throughout NYC yields a Root Mean
98 Square Error (RMSE) of 0.075 m in elevation. Comparison with 200 building corner
99 points yields a RMSE of 0.33 m horizontal error ((Ahern and Ahn 2011)). Extraction of
100 first and last returns from the full waveform LiDAR allowed for better discrimination of
101 true ground elevations under tree canopies and semi-penetrable land cover types. The
102 LDSM measures tops of buildings, trees and infrastructure, as well as ground elevations
103 where sufficient skyview exists. Known ground elevations were used to extract the DEM
104 from the LDSM and last returns. The LDEM ground elevations under buildings are
105 estimates based on surrounding true ground elevations. Some residual building footprints
106 remain in the LDEM (Fig. 1) but their amplitude is generally < 1 m.

107

108 The GDEM2 and SRTM (v2.1) DEMs were obtained from the USGS in the form of 1 arc
109 second (1" = ~28 m at 40°N) resolution geographic grids in the WGS84 horizontal and
110 EGM96 vertical reference systems. The LDEM and LDSM were spatially averaged with
111 a 1" Gaussian kernel and sampled at points coincident with the global DEMs along 6
112 transects (Fig. 1). Transects were chosen to maximize length, relief and diversity of
113 coastal environments. For each transect, two adjacent rows (or columns) of the global
114 DEMs were compared to check consistency of spectral estimates for similar (but not
115 identical) realizations of the terrain. Transect WE1 extends westward from the East
116 River through midtown Manhattan where neither global DEM was able to register
117 accurate elevations because of the considerable height variability resulting from tall
118 buildings, as can be seen in the LiDAR DSM. The NUM files that accompany SRTM v3
119 indicate that infill elevations were used to fill coverage gaps in midtown Manhattan and
120 one pol on Jamaica Bay but not any other part of the transects selected for analysis. We
121 exclude midtown from our spectral analyses but include it in Figure 1 to illustrate the
122 infill elevations used to fill the gaps in DEM coverage. Within the NYC study area, the

123 SRTM grid used between one and four (mode = 3) acquisitions and GDEM2 used
124 between one and twelve (mode = 7) acquisitions.

125

126 **Analysis and Results**

127

128 We use scatterplots and moments of difference distributions to quantify the point-to-point
129 correspondence between the global DEMs and the 14,572 LiDAR elevations. The results
130 show closer agreement between LDEM and SRTM than between LDEM and GDEM2
131 (Fig. 2). In the LDEM and SRTM comparison, 25% of the SRTM elevations
132 underestimate the LiDAR ground elevations while almost all of the GDEM2 elevations
133 overestimate the LiDAR ground elevations. An important difference between global
134 DEMs is observed at the lowest elevations where GDEM2 always overestimates LDEM
135 but SRTM often underestimates LDEM (Fig. 2). This difference is also illustrated by the
136 large, low elevation wetlands (e.g. Jamaica Bay and New Jersey Meadowlands) in Figure
137 1. The 1st and 2nd moments of the difference distributions give the bias (μ) and
138 uncertainty (σ) of each global DEM relative to the corresponding LiDAR model. Both
139 global DEMs have overall positive bias relative to the LiDAR DEM but GDEM2 bias
140 and uncertainty are much greater than those of SRTM (Fig. 2).

141

142 We conduct cross-spectral analyses of the four elevation models along all 6 transects to
143 assess the scale-dependence of correlation. Power spectral density, cross-spectral phase
144 and spectral coherency are estimated using the multitaper method (Thomson 1982) with
145 adaptive weighting (Percival and Walden 1993) and a time-bandwidth product of eight.
146 Multitaper estimation reduces the bias resulting from spectral leakage while minimizing
147 the information loss inherent in the use of conventional tapers and avoiding the need for
148 prewhitening (Thomson, 1982). Adaptive weighting minimizes the mean square error of
149 the spectral estimates by determining the weights for each taper using an iterative
150 procedure that accounts for the (nonwhite) spectral content of the data (Percival and
151 Walden 1993).

152

153 The power spectral density estimates show the relative amount of variance over a range
154 of spatial scales (wavelengths). Power spectra of elevation data are often used to
155 quantify scale dependent variance as a proxy for topographic roughness (e.g. (Fox and
156 Hayes 1985). The spectral shape and roll-off of each transect are functions of the
157 elevation profile roughness (Fig. 3, top panels). For example, LDSM consistently has
158 more power than LDEM at short wavelengths because the land cover upper surface (e.g.
159 buildings and trees) is rougher than the underlying topography, especially in developed
160 areas with multi-story buildings. GDEM2 consistently has greater power than SRTM at
161 short wavelengths, perhaps because of noise in GDEM2 resulting from spectral
162 heterogeneity of land cover imaged by ASTER. Spectral power levels for all four
163 elevation models are similar for length-scales $> \sim 1$ km, but begin to diverge at length-
164 scales of 0.5 – 1.0 km, where the relief associated with land cover (e.g. buildings and
165 trees) has greater variance than the smoother underlying topography. We refer to this
166 wavelength where the DSM and DEM separate (shown by arrows in Figure 3) as the
167 surface-elevation divergence scale (λ_D).

168

169 The cross-spectral analysis (Figure 3, bottom panels) indicates that both global DEMs
170 become incoherent at spatial scales $< \sim 0.5$ km. Coherency, which estimates correlation
171 as a function of spatial wavelength, between GDEM2 and both LiDAR models begins to
172 roll-off for wavelengths $< \sim 3$ km, while the coherency between SRTM and LDEM begins
173 to roll-off for wavelengths $< \sim 1$ km. We define the correlation scale (λ_c) between two
174 models as the length-scale at which the coherency drops below 0.5; a threshold value
175 representing a signal-to-noise ratio of one (Bendat and Piersol 2010). We find that the
176 correlation scale for GDEM2 relative to both LiDAR models is between 1.4 and 0.7 km,
177 while the correlation scale for SRTM relative to LDEM is between 0.7 and 0.4 km.
178 These correlation scales (λ_c) are similar to the surface-elevation divergence scales (λ_D)
179 observed in the power spectra (Fig. 3). This indicates that the correlation scales where
180 agreement among DEMs disappears occurs at divergence scales where the surface
181 roughness of the land cover exceeds the roughness of the underlying terrain.

182
183 The cross-spectral analysis suggests that structure at scales $< \sim 1$ km is as likely to be
184 noise as true elevation in both global DEMs. To illustrate this, we filter all four DEMs
185 for profile NS2 to remove incoherent structure at wavelengths < 1 km (Fig. 4). The
186 filtered profiles are in much closer agreement than the raw profiles, especially for the
187 SRTM and LDEM, and the positive bias of GDEM2 is readily apparent.

188
189

190 **Implications**

191

192 Our results quantify the correlation scales of the GDEM2 and SRTM global elevation
193 models for both developed and natural coastal environments in NYC. In general, we find
194 that the global DEMs accurately resolve features with length scales $> \sim 1$ km, but at
195 shorter length-scales noise overwhelms the elevation signal. The correlation scale for
196 SRTM extends to shorter length-scales (~ 500 m) compared to GDEM2 (~ 1 km), and
197 GDEM2 exhibits a systematic, ~ 8 m positive bias throughout the study area (Figs. 1 & 2).
198 This may be due, in part, to vertical reference error in GDEM2.

199

200 The power spectra and correlation scales vary somewhat among the profiles, with most
201 differences occurring at spatial scales finer than ~ 1 km where the land cover and the
202 underlying topography signals begin to diverge. The accuracy of the global DEMs begins
203 to deteriorate at about the same length-scale where heterogeneous land cover associated
204 with developed environments becomes the dominant signal. The consistently higher
205 variance (power) and lower coherencies we observe for GDEM2 compared to SRTM for
206 length-scales of 0.5 – 3 km suggest that heterogeneous land cover in developed areas
207 introduces more noise into GDEM2 elevation estimates compared to SRTM elevation
208 estimates.

209

210 The scale and diversity of urban land cover poses challenges to stereography using
211 decameter resolution imagery. Comparative multi-scale analyses of meter to decameter
212 resolution optical imagery of urban environments reveal considerable intra-urban spectral
213 diversity with characteristic spatial scales of 20 to 50 m (Small 2009). The spectral
214 diversity and scale-dependent spectral mixing endemic to urban land cover violates the

215 assumptions of spectral homogeneity and Lambertian scattering that are implicit to
216 stereography (Lang and Welch 1999). As a result, the 20-30 m spatial resolution of the
217 ASTER sensor is not well suited to stereography in heterogeneous urban environments
218 with abundant specular reflectors. However, this does not imply that GDEM2 is not
219 well-suited to more spectrally homogeneous environments with greater topographic
220 relief. GDEM2 is an important complement to SRTM because it provides coverage at
221 higher latitudes and in areas of very steep terrain and sand dunes where SRTM often
222 contains voids (Farr 2006).

223
224 The correlation scales of the SRTM and LDEM are consistent with, but larger than,
225 previous studies that quantify scale-dependent resolution of SRTM. The continental-
226 scale structure function analyses conducted by Rodriguez et al. (2006) find height error
227 correlation functions dropping rapidly for scales $< \sim 500$ m. The cross spectral analysis of
228 LiDAR and SRTM for Mojave Desert terrain conducted by Smith and Sandwell (2003)
229 found average spectral coherence of 0.5 at scales of ~ 200 m. The effective spatial
230 resolution of the stereographic and synthetic aperture radar algorithms are generally
231 coarser than the 30 m grid resolutions but finer than the 0.5 to 1 km correlation scales
232 observed in this study. The larger correlation scales found in this study suggest that
233 global DEMs may have lower effective spatial resolution (or that noise levels are
234 correspondingly higher) in developed coastal environments compared to continental
235 averages and mountainous, high desert, environments. We conjecture that the lower
236 effective spatial resolutions of both global DEMs in developed coastal environments is a
237 result (at least in part) of the heterogeneity of land cover with characteristic spatial scales
238 comparable to the IFOV of the sensors used for the global models.

239
240 Overall, both global DEMs are well within their stated accuracy specifications and appear
241 to have closer agreement to measured elevations than in some previous studies cited
242 above. However, in addition to the apparently random errors discussed above, we do
243 observe some systematic errors when comparing full 2D DEMs at 1" resolution. The
244 largest and most obvious errors in both models occur in areas of high relief at pixel
245 scales; (e.g. buildings in Manhattan). Both global DEMs overestimate ground elevation
246 and underestimate building top heights by > 10 m in most areas where buildings exceed
247 tree height. Consistent with the findings of (Hofton et al. 2006), SRTM overestimates
248 elevation in areas of dense, closed canopy forest where the phase center lies within the
249 canopy. GDEM2 also overestimates surface elevations in some wetlands.

250

251 **Acknowledgements**

252 This research was supported by the Office of Naval Research (grant N000-14-11-1-0653
253 to C.S.). We thank Tom Farr and Bob Crippen for helpful comments and suggestions.
254 ASTER GDEM is a product of METI and NASA.

255

256 **References**

257

258 Abrams, M., Bailey, B., Tsu, H., & Hato, M. (2010). The ASTER global DEM.
259 *Photogrammetric Engineering and Remote Sensing*, 76, 344-348

260 Ahern, S.C., & Ahn, H.J. (2011). Quality assurance and potential applications of a
 261 high density LiDAR data set for the City of New York, Proceedings of ASPRS, (p.
 262 9).

263 Bendat, J.S., & Piersol, A.G. (2010). *Random Data: Analysis and Measurement*
 264 *Procedures, 4th Edition: Wiley*

265 Carabajal, C.C., & Harding, D.J. (2006). SRTM C-band and ICESat laser altimetry
 266 elevation comparisons as a function of tree cover and relief. *Photogrammetric*
 267 *Engineering and Remote Sensing, 72, 287-298.*

268 Farr, T.G. (2006). Voids in SRTM data caused by sand dunes. In, *EUSAR 2006 -*
 269 *6th European Conference on Synthetic Aperture Radar.* Dresden, Germany

270 Farr, T.G., Rosen, P., Caro, E., Crippen, R., Duren, R., Hensley, S., Kobrick, M.,
 271 Paller, M., Rodriguez, E., Roth, L., Seal, D., Shaffer, S., Shimada, J., Umland,
 272 J., Werner, M., Oskin, M., Burbank, D., & Alsdorf, D. (2007). The Shuttle Radar
 273 Topography Mission. *Reviews of Geophysics, 45, 1-33*

274 Fox, C.G., & Hayes, D.E. (1985). Quantitative methods for analyzing the
 275 roughness of the seafloor. *Reviews of Geophysics, 23, 1-48*

276 Gesch, D., Oimoen, M., Zhang, Z., Meyer, D., & Danielson, J. (2012).
 277 VALIDATION OF THE ASTER GLOBAL DIGITAL ELEVATION MODEL
 278 VERSION 2 OVER THE CONTERMINOUS UNITED STATES. In, *2012 XXII*
 279 *ISPRS Congress* (pp. 281-286). Melbourne, Australia: ISPR

280 Gorokhovich, Y., & Voustianiouk, A. (2006). Accuracy assessment of the
 281 processed SRTM-based elevation data by CGIAR using field data from USA
 282 and Thailand and its relation to the terrain characteristics. *Remote Sensing of*
 283 *Environment, 104, 409-415*

284 Hofton, M., Dubayah, R., Blair, J.B., & Rabine, D. (2006). Validation of SRTM
 285 Elevations Over Vegetated and Non-vegetated Terrain Using Medium
 286 Footprint Lidar. *PHOTOGRAMMETRIC ENGINEERING & REMOTE*
 287 *SENSING, 72, 279-285*

288 Hvidegaard, S.M., Sorensen, L.S., & Forsberg, R. (2012). ASTER GDEM
 289 validation using LiDAR data over coastal regions of Greenland. *Remote*
 290 *Sensing Letters, 3*

291 Lang, H.R., & Welch, R. (1999). ATBD-AST-08 ALGORITHM THEORETICAL
 292 BASIS DOCUMENT FOR ASTER DIGITAL ELEVATION MODELS
 293 (STANDARD PRODUCT AST14). In: NASA

294 Meyer, D.J., Tachikawa, T., Abrams, M., Crippen, R., Krieger, T., Gesch, D., &
 295 Carabajal, C. (2012). SUMMARY OF THE VALIDATION OF THE SECOND
 296 VERSION OF THE ASTER GDEM. In, *2012 XXII ISPRS Congress* (pp. 291-
 297 293). Melbourne, Australia: ISPRS

298 Percival, D.B., & Walden, A.T. (1993). *Spectral Analysis for Physical Applications.*
 299 Cambridge, England: Cambridge University Press

300 Rodriguez, E., Morris, C.S., & Belz, J.E. (2006). A global assessment of the
 301 SRTM performance. *Photogrammetric Engineering & Remote Sensing, 72,*
 302 *249-260*

303 Small, C. (2009). The Color of Cities: An Overview of Urban Spectral Diversity. In
304 M. Herold & P. Gamba (Eds.), *Global Mapping of Human Settlements* (pp. 59-
305 106): Taylor and Francis
306 Smith, B., & Sandwell, D. (2003). Accuracy and resolution of shuttle radar
307 topography mission data. *Geophysical Research Letters*, 30, 20-21-24
308 Tachikawa, T., Hato, M., Kaku, M., & Iwasaki, A. (2011). Characteristics of ASTER
309 GDEM version 2. In, *International Geoscience and Remote Sensing*
310 *Symposium (IGARSS)* (pp. 3657-3660.): IEEE
311 Tadono, T., Takaku, J., & Shimada, M. (2012). VALIDATION STUDY ON ALOS
312 PRISM DSM MOSAIC AND ASTER GDEM 2. In, *2012 XXII ISPRS Congress*
313 (pp. 193-198). Melbourne, Australia: ISPRS
314 Thomson, D. (1982). Spectrum estimation and harmonic analysis. *Proceedings of*
315 *the IEEE*, 70, 1055–1096.
316
317
318

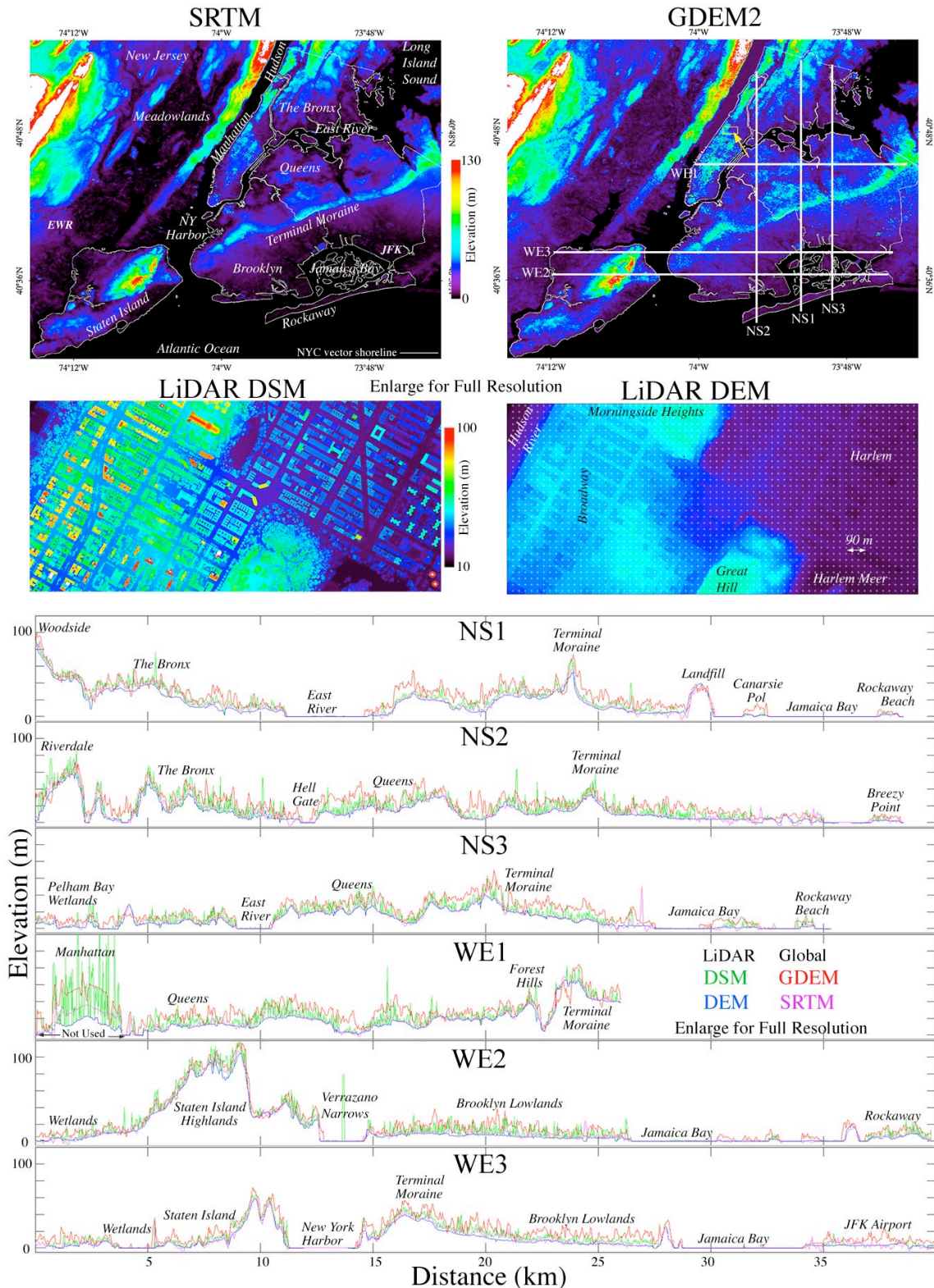


Figure 1. Comparison of global elevation models (top) with full resolution samples of the LiDAR DSM and DEM (center) and coregistered profiles from each model used for analysis. Location of LiDAR sample shown by arrow and box on GDEM2 map.

319
320

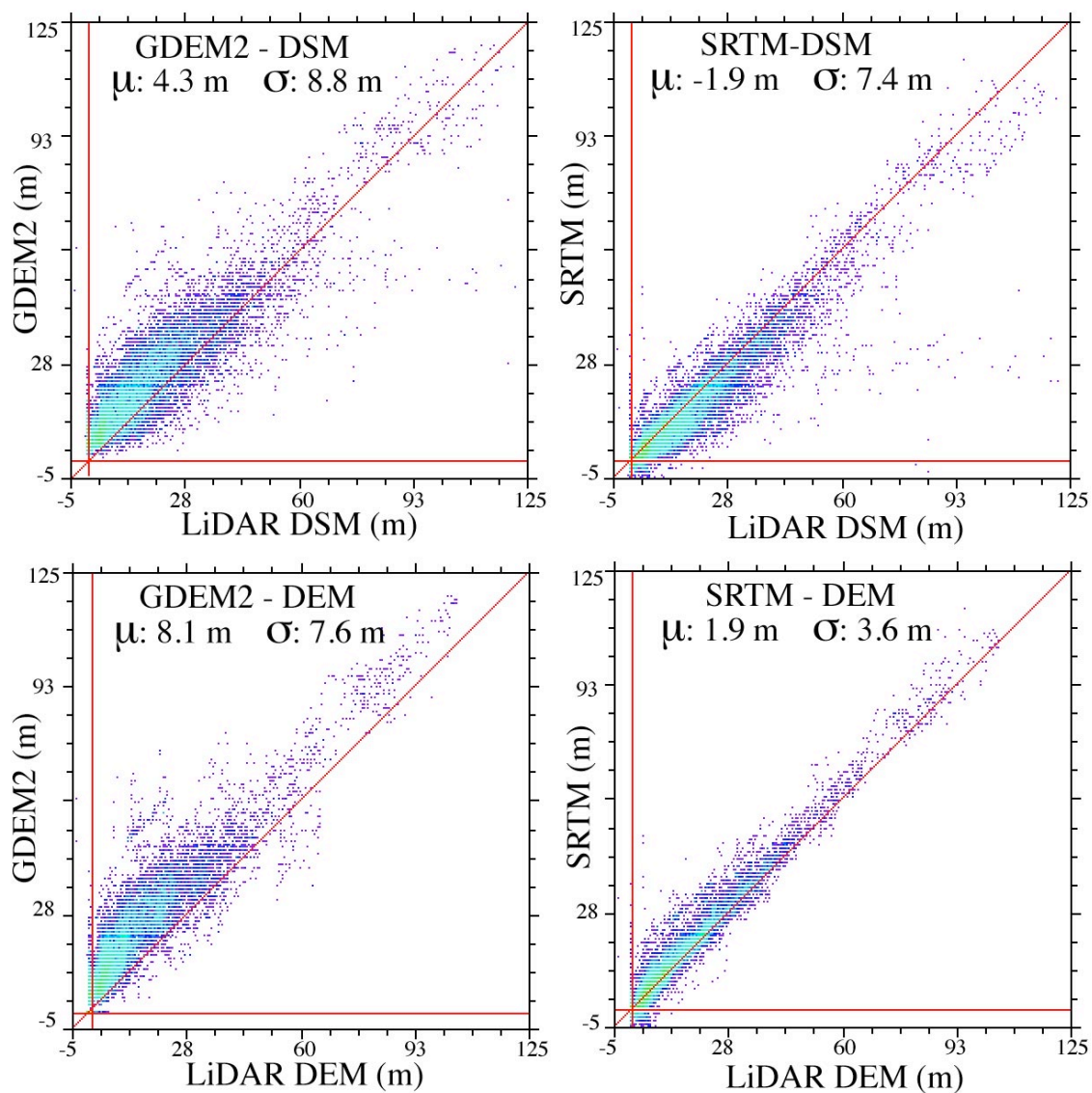


Figure 2. Density shaded scatterplots comparing global elevation models with LiDAR elevations. Distributions of 14,572 coregistered elevations are derived from 6 adjacent pairs of profiles sampled at 30 m postings along transects shown in Fig. 1. Moments of distributions of differences between global models and LiDAR quantify model bias (μ) and uncertainty (σ). Warmer colors indicate greater number of points.

321
322

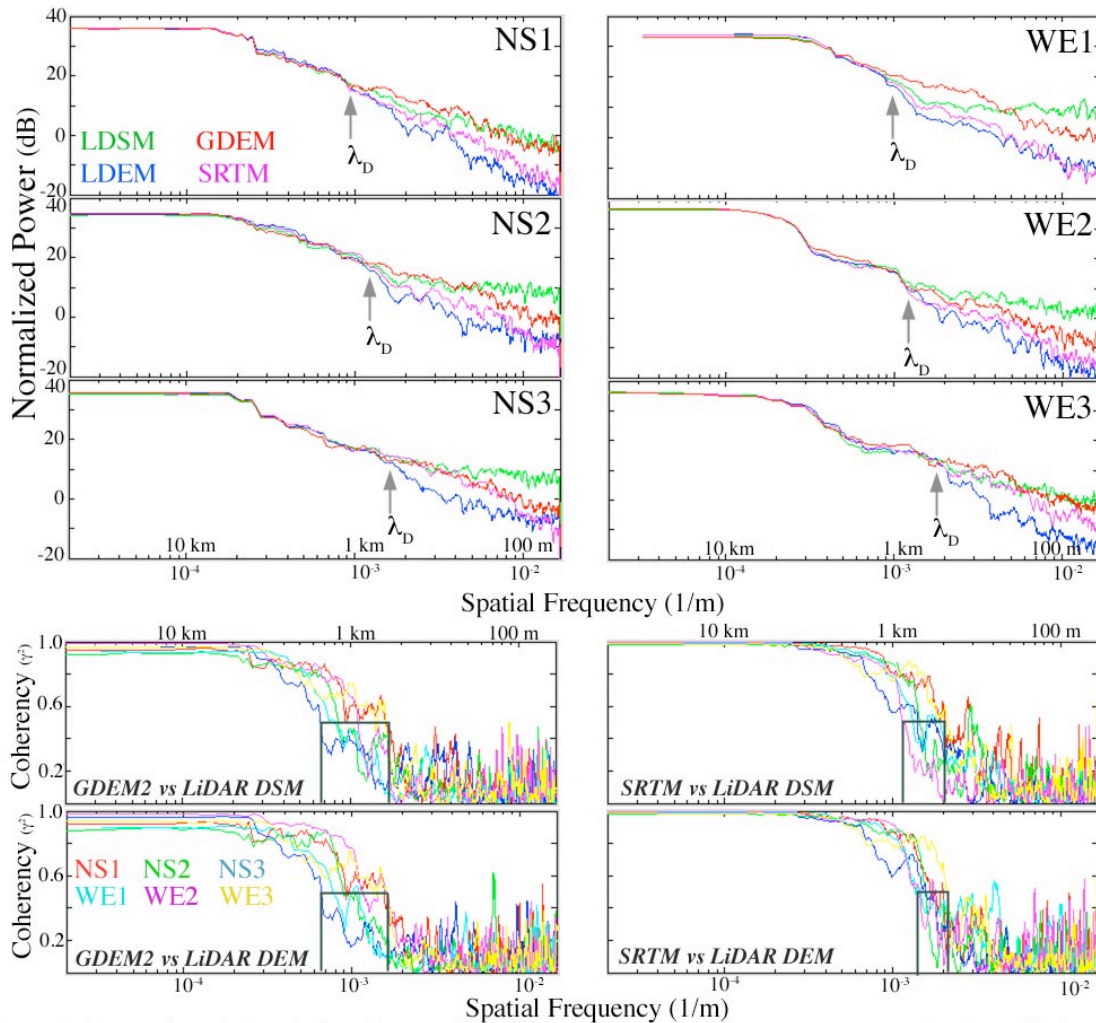


Figure 3 Spectral analysis of elevation models along coastal transects. Power spectra (top) are distinct for each of the 6 transects but show similar relationships among models for all transects. Spectral slopes at higher frequencies show rougher “tops” (DSM) and smoother “bottoms” (DEM). Spectra diverge for $\lambda < \sim 1$ km for all profiles but coherency begins to deteriorate at longer λ for GDEM2 than SRTM. The correlation scales λ_c where coherency reaches 0.5 (boxes) corresponds to the divergence scale λ_D where the roughness of land cover begins to exceed the roughness of the underlying terrain (arrows).

323
324

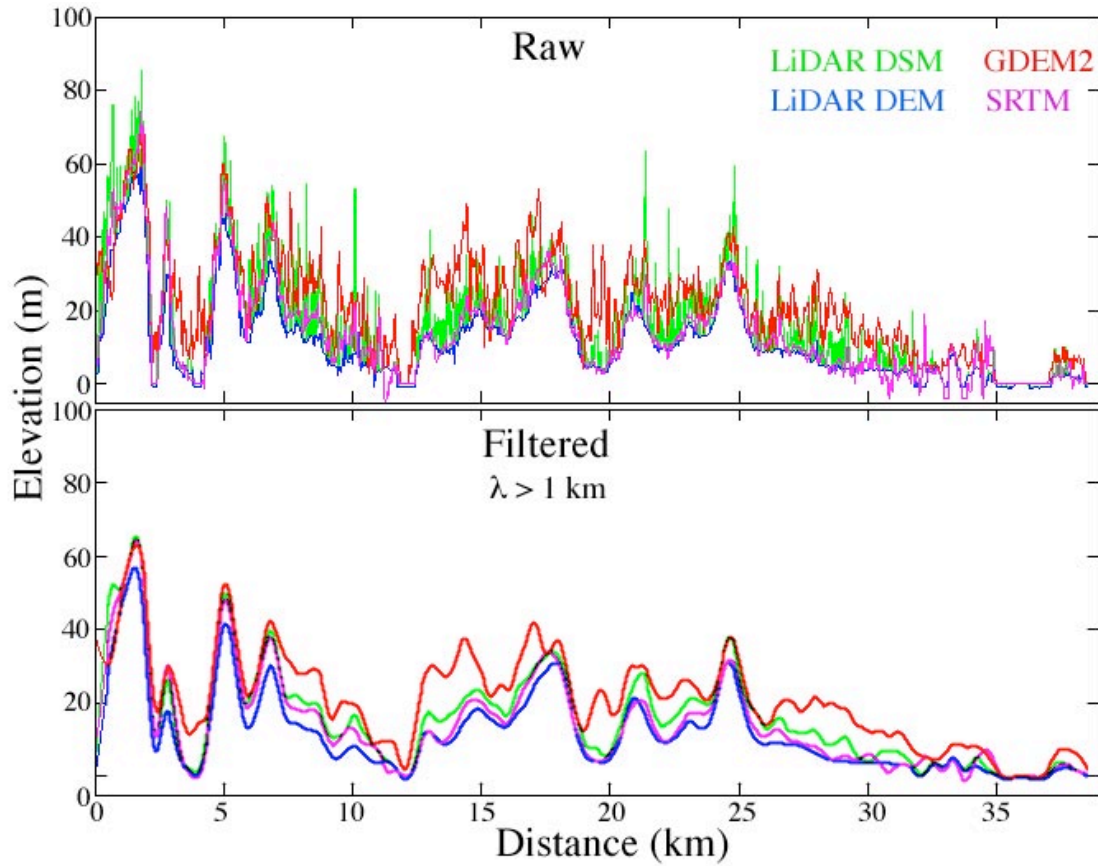


Figure 4 Comparison of raw and filtered elevations. Profile NS2 illustrates the effects of removal of incoherent short wavelength ($\lambda < 1$ km) variance from all 4 models. The LiDAR DEM and SRTM agree well in most areas. The GDEM2 model retains some short wavelength ($\lambda < \sim 3$ km) artifacts and positive bias relative to the LiDAR DSM. Note GDEM amplification of short λ features of DSM.

325